The Structure−Function Relationship of Hemoglobin in Solution at Atomic Resolution

Jonathan A. Lukin and Chien Ho*

Department of Biological Sciences, Carnegie Mellon University, Pittsburgh, Pennsylvania 15213

Received February 28, 2003

Contents

1. Introduction

Hemoglobin (Hb) is an essential component of the circulatory system of vertebrates. Its chief physiological function is to transport oxygen from the lungs to the tissues. For reviews of the structure−function relationship in hemoglobin, see Dickerson and Geiss,[1] Ho,[2] and Ho and Lukin.[3] Human normal adult hemoglobin (Hb A) is one of the most studied proteins and has served as a model or paradigm for multimeric allosteric proteins. Hemoglobin is a useful system for testing a basic premise of structural biology, which holds that the functional properties of a protein can be explained in terms of its structure and dynamic behavior on the atomic scale. Since the first crystal structures of Hb A were determined by Perutz and colleagues in the 1960s, extensive efforts have been devoted to elucidating the relationship of hemoglobin's structure with its physiologically important properties, including the cooperative binding of oxygen, and the control of oxygen affinity by pH (the Bohr effect) and allosteric effectors such as 2,3-bisphosphoglycerate (2,3-BPG). Despite these efforts, the detailed structural basis of these properties is not fully understood, and some aspects remain controversial. Much of our current understanding of Hb A has been obtained with reference to X-ray crystal structures. However, since the protein performs its physiological functions in the solution state, it is useful to investigate its structure−function relationships in solution, using techniques including infrared, resonance Raman, and nuclear magnetic resonance (NMR) spectroscopies.

One-dimensional (1D) ^{1}H NMR spectroscopy has been used extensively to study the behavior of Hb in solution by following the response of assigned ^{1}H resonances to varied conditions, and to modifications of the protein.[2,4,5] This technique is limited, however, by the broadening of resonance lines observed for large proteins such as Hb, which results in a degenerate ^{1}H NMR spectrum, where only a few resonances are well-resolved. The spectral resolution, and consequently the amount of structural and dynamic information obtainable, can be greatly enhanced by the application of multidimensional, multinuclear NMR to isotopically labeled protein samples. Labeling of Hb A with ^{2}H, ^{15}N, and ^{13}C has become feasible through the development of a bacterial expression system for this protein.[6,7] Expression of hemoglobin in *Escherichia coli* also makes it possible to produce any desired mutant recombinant hemoglobin (rHb), by site-directed mutagenesis. Much insight into the structure−function relationships of Hb has been gained by investigating the properties of rHbs where amino acid substitutions have been made at key residues.[8−14] This article will review recent progress in understanding the structure−function relationships of hemoglobin in solution, emphasizing results obtained by NMR spectroscopy.

2. Structure

2.1. Sequence, Secondary Structure, and Globin Fold

The structure of a protein is traditionally described in terms of four levels of organization.[15] The primary structure is the amino acid sequence of the polypeptide. Secondary structure refers to the local spatial arrangement of amino acid residues, in terms of α-helices, β-strands, turns, and loops. The overall three-dimensional fold of a polypeptide chain is referred to as the tertiary structure. Quaternary structure refers to the spatial arrangement of subunits. Hb A is a tetrameric protein with a molecular weight of 64 500 Da, consisting of two identical α-chains of 141 amino acids each, and two identical β-chains of 146 amino acids each. The secondary

* To whom correspondence should be address. Telephone: 412-268-3395. Fax: 412-268-7083. E-mail: chienho@andrew.cmu.edu.

10.1021/cr940325w CCC: $48.50
Published on Web 02/07/2004

Dr. Ho did his undergraduate training at Williams College and received his B.A. degree in chemistry in 1957. He then went to Yale University for his graduate work in physical chemistry with Julian M. Sturtevant and received his Ph.D. degree in 1961. From 1960–61, he was a Research Chemist for Linde Company, Union Carbide Corporation, working on the liquid nitrogen temperature preservation of human blood. From 1961–64, he did postdoctoral research with George Scatchard and Jancinto Steinhardt in Department of Chemistry and with David F. Waugh in the Department of Biology, Massachusetts Institute of Technology. From 1964–79, he was an assistant professor, associate professor, and professor of molecular biology at the University of Pittsburgh. In 1979, he joined Carnegie Mellon University as the head and professor of the Department of Biological Sciences. He is currently Alumni Professor of Biological Sciences and the Director of the Pittsburgh NMR Center for Biomedical Research. His research goal is to understand the relationship between structure and function in biological systems by correlating information obtained from biochemical, biophysical, and molecular biological techniques. His current research is focused in two areas. The first centers on a study of human normal and abnormal hemoglobins in order to correlate the structure, dynamics, and function of hemoglobin in solution at atomic resolution. The second centers on the application of magnetic resonance imaging (MRI) and spectroscopy (MRS) to biomedical systems. He is currently developing noninvasive techniques to monitor the migration/accumulation of immune cells in vivo by MRI as a means to detect early signs of graft rejection following solid organ transplantation.

Jonathan Lukin did his undergraduate work in physics at Case Western Reserve University, graduating in 1984. He then performed doctoral work at Carnegie Mellon University, studying low-temperature magnetic ordering in solids under S. A. Friedberg. A postdoctoral appointment with Chien Ho followed, during which he became interested in the structure–function relationship in proteins, and he investigated such relationships in glutamine-binding protein and hemoglobin using nuclear magnetic resonance (NMR) spectroscopy. His interests also include experimental and computational methods for protein resonance assignment and solution structure determination.

structure of each polypeptide subunit of Hb A is predominantly α-helical. Hb A does not contain any β-strands, or disulfide bonds. Curiously, the amino acid isoleucine is also absent. A β-chain of Hb A includes eight helical segments, designated A−H. An α-chain is very similar but lacks a D helix. In a nomenclature common to the globin proteins, each amino acid residue is designated by its position in a helix or interhelical segment. For example, α87His and β92His are both F8His, the eighth residue in the F helix in their respective subunits.

Each subunit or chain of Hb A adopts a three-dimensional structure, called the globin fold, similar to that of the related, monomeric protein myoglobin (Mb). This fold is an arrangement of the helices which forms a pocket that encloses and binds a heme prosthetic group. In each subunit, the polypeptide is linked to the heme by a covalent bond between the $N\epsilon_2$ atom of the F8His residue (the proximal histidine), and the heme iron. This iron atom, in the ferrous state, is capable of reversibly binding gaseous ligands including oxygen, carbon monoxide, and nitric oxide. These ligands bind at the distal side of the heme plane, opposite to the proximal His, resulting in octahedral coordination of the iron. In a solution of isolated heme groups, the formation of a complex of oxygen sandwiched between two hemes results in the rapid oxidation of iron to the ferric state, which cannot bind oxygen. The polypeptide chains of Hb and Mb create a hydrophobic environment, which prevents the formation of this complex, allowing the heme to reversibly bind oxygen over long periods of time.

2.2. Quaternary Structure and Conformations

As noted earlier, Hb A consists of two identical α-chains and two identical β-chains. Thus, Hb A can be thought of as a dimer of αβ dimers. The $\alpha_1\beta_1$ and $\alpha_2\beta_2$ dimers are related by a 2-fold axis of symmetry that runs down a water-filled cavity in the center of the protein (Figure 1A). Thus, the $\alpha_1\beta_1$ and $\alpha_2\beta_2$ subunit interfaces are identical, as are the $\alpha_1\beta_2$ and $\alpha_2\beta_1$ subunit interfaces.[1] The arrangement of subunits (i.e., the quaternary structure) of Hb depends on the ligation state of the protein and is related to the physiologically vital property of cooperativity.[16] The two classical quaternary structures are the T (tense) form for the low-affinity deoxy-Hb and the high-affinity R (relaxed) form for the high-affinity liganded Hb. These structures were determined by Perutz and colleagues from X-ray crystallographic studies of high-salt crystals some 30 years ago and form the basis of Perutz's stereochemical mechanism for the cooperative oxygenation of Hb.[17] More recently, however, a second, distinctly different crystal structure for Hb A was solved and designated R2. The R2 conformation has been seen in carbonmonoxy-Hb A in low salt conditions at pH 5.8,[18] as well as in cyanomet-Hb A crystallized under physiological salt and pH conditions.[19] Geometric analysis indicates that the R conformation lies along the pathway between T and R2, and that the difference in structure between R and R2 is comparable in magnitude to that between T and R.[20,21] This observation raises the question of whether R or R2 represents the true final liganded state in solution.[22]

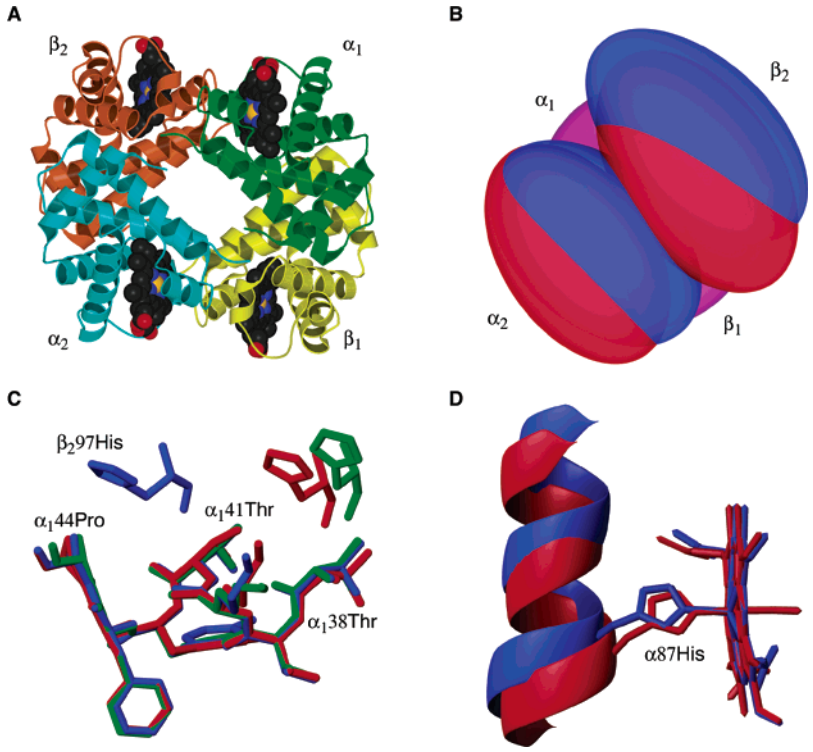

Figure 1. Illustrations of Hb A structure produced using the graphics programs MOLMOL[80] and MolScript.[81] Coordinates of Hb A in the T (deoxy), R (CO), and R2 (CO) conformations were obtained from Protein Databank files 1A3N, 1IRD, and 1BBB, respectively. (A) Deoxy-Hb A, viewed along the 2-fold symmetry axis, showing the water-filled central cavity. (B) Illustration of the reorientation of $\alpha\beta$ dimers in the T-to-R transition. Each protein subunit is shown schematically as an ellipsoid. The $\alpha_1\beta_1$ dimers of the two conformations, shown in violet toward the rear of the figure, have been superimposed at the $\alpha_1\beta_1$ interface. The α_2 and β_2 subunits of deoxy and carbonmonoxy-Hb are shown in blue and red, respectively. To a first approximation, the $\alpha_2\beta_2$ dimer rotates as a rigid unit. (C) Switch region of the $\alpha_1\beta_2$ interface of Hb A in the T, R, and R2 conformations, shown in blue, red, and green, respectively. Here, the backbone atoms of residues 38−44 in the α_1 subunit have been superimposed, to illustrate the relative motion of $\beta_2$97His. (D) The α-subunit hemes, proximal histidines, and F helices of deoxy-Hb (blue) and carbonmonoxy-Hb (red), with hemes superimposed.

The $\alpha_1\beta_1$ interface is stabilized by a large number of packing contacts and hydrogen bonds and is nearly identical in the T, R, and R2 conformations.[18,23,24] Thus, to a good approximation, the $\alpha_1\beta_1$ and $\alpha_2\beta_2$ dimers move as rigid units during the T to R transition. In contrast to the fixed $\alpha_1\beta_1$ and $\alpha_2\beta_2$ interfaces, the $\alpha_2\beta_1$ and $\alpha_1\beta_2$ interfaces undergo significant changes upon ligation of Hb. During the T to R transition, the $\alpha_1\beta_1$ dimer rotates by 15° with respect to the $\alpha_2\beta_2$ dimer, about an axis passing through the α-subunits;[16] see Figure 1B. The R to R2 transition is characterized by a further rotation, by approximately 11°, about a nearby axis.[20,21] The regions of the $\alpha_1\beta_2$ interface near the pivot point, within the FG corner of the α-chain and the C helix of the β-chain, remain in contact and are termed the "hinge" or "flexible joint". Farther from the pivot point, the largest conformational change occurs in the "switch region", shown in Figure 1C, where residue $\beta_2$97His is displaced by one turn of the C helix of the α_1-chain, from the groove between the side-chains of α_1Thr41 and α_1Pro44, to between α_1Thr38 and α_1Thr41. Ligation of Hb also disrupts several hydrogen bonds and salt bridges between the α_1- and β_2-subunits.[1,16]

3. Structure–Function Relationships in Solution

3.1. Ligand Discrimination

An important function of both hemoglobin and myoglobin is to modulate the affinity of the heme for ligands such as O_2, CO, and NO. The relative affinity of CO and O_2 is expressed in terms of the ratio of equilibrium binding constants $M \equiv K_{CO}/K_{O2}$, which is approximately 20 000 for unencumbered model heme compounds in organic solvents.[25] This ratio is so very high that small amounts of CO, which is produced endogenously by the catabolic breakdown of heme itself, would be fatally toxic.[26] Fortunately, the binding affinity of O_2 relative to that of CO is strongly enhanced in Hb A and Mb, which reduce the value of M to about 250 and 25, respectively.[27] Two different mechanisms have been proposed to account for the discrimination against CO binding in heme proteins. The first explanation relied upon early X-ray crystal structures, which indicated that both CO and O_2 adopted a bent orientation when bound to Mb. However, it was known that CO and O_2 have different geometric preferences when bound to heme; while O_2 is naturally bent, CO prefers to bind in an upright fashion. Thus, Collman and co-workers[26] proposed that distal amino acid residues in Mb discriminate against CO binding, by forcing the bound CO into an unfavorable, bent orientation. This steric hindrance mechanism was disputed by Spiro and co-workers,[28−30] who pointed out that a large degree of Fe−CO bending was inconsistent with observed vibrational spectra and would require stronger localized steric forces than a polypeptide is capable of exerting. More recent, high-resolution

X-ray structures of both MbCO[31,32] and HbCO A (PDB entry 1IRD) suggest a modest off-axis distortion of the ligand, which can be realized at a lower energetic cost if tilting of the Fe−C bond and buckling of the heme occur together with Fe−C−O bending. The strongly bent Fe−C−O geometry of the early X-ray crystal structure is now considered a likely result of partial oxidation of the protein to met-Mb during the course of data collection.[30,33]

Time-resolved IR polarization spectroscopy,[34] as well as a joint analysis of NMR, ^{57}Fe Mossbauer, and IR data,[35] indicate an upright, perpendicular geometry of the CO group bound to Mb. Any remaining discrepancy between this model and recent X-ray structures is reconciled by density functional theory calculations,[36] which show that the transition dipole of the C−O stretching IR band is not coincident with the C−O bond vector, but lies between the Fe−C bond vector and the heme perpendicular. The minimum energy structure consistent with the measured IR transition dipole is slightly tilted and bent, giving an off-axis displacement of the oxygen atom that is within the distribution seen in MbCO crystal structures. Steric distortion may still play a part in lowering the CO affinity of Mb and Hb, as the binding of the ligand in a nearly upright orientation may require displacement of distal residues[37] or concerted motion of protein helices.[31] However, analysis of kinetic and equilibrium binding constants of a large number of Mb mutants indicates that steric inhibition accounts for only about 0.5 kcal/mol, out of a total of ∼3.5 kcal/mol of discrimination against CO binding.[25,30]

Rather than steric constraints hindering the binding of CO, an alternative explanation for the reduced value of M in heme proteins is that electrostatic interactions and hydrogen-bonding favor the binding of O_2. Back-donation of electrons from the heme Fe(II) occurs in complexes of heme with either ligand, but the transfer of charge is much greater for O_2 than for CO.[25] Thus, O_2 can form a strong H-bond with the distal histidine (E7His), but CO forms (at most) a very weak one. In Mb, a weak H-bond to the bound CO is suggested by D_2O sensitivity of the FeCO vibrations,[38] while a strong H-bond to O_2 has been observed by neutron diffraction.[39] The question of whether an H-bond to the distal histidine exists in hemoglobin in solution can be addressed by NMR spectroscopy. Two-dimensional (2D) NMR spectroscopy is ideally suited to the study of histidines in ^{15}N-labeled proteins, because $^{15}N\delta_1$ and $^{15}N\epsilon_2$ resonate at characteristic chemical shifts, far removed from those of the backbone amides and other amino acid side-chains.[40]

In a heteronuclear multiple quantum coherence (HMQC) spectrum, the histidyl side-chains produce a pattern of cross-peaks indicative of the tautomeric state of the residue[41] (see Figure 2). The protonated ^{15}N of a histidyl imidazole ring has a chemical shift of roughly 160 ppm, while the bare ^{15}N resonates further downfield, around 250 ppm. In general, both nitrogens in the ring are coupled to both carbon-bound protons, resulting in a rectangular pattern of four cross-peaks in the HMQC spectrum;[42,43] the

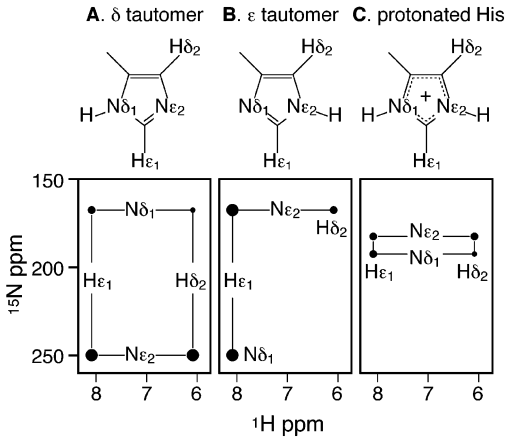

Figure 2. Schematic diagram showing the expected (^{1}H,^{15}N)-HMQC spectrum of the imidazole-ring for each of the three possible protonation states of a histidyl residue. Large, medium, and small black circles indicate strong, medium, and weak cross-peaks, respectively. Note that, for the charged species (panel C), either of the nitrogens could resonate downfield of the other; the assignment must be made on the basis of the relative weakness of the ($N\delta_1$, $H\delta_2$) cross-peak. Reproduced with permission from ref 7. Copyright 2000 Biophysical Society.

three cross-peaks that correspond to two-bond couplings will be relatively intense. A less intense or missing cross-peak is diagnostic of the weak three-bond ($H\delta_2$, $N\delta_1$) coupling. A cross-peak corresponding to the direct, one-bond coupling between a side-chain ^{15}N and its bonded ^{1}H is observed only if the proton is protected from rapid exchange with solvent, either by a hydrogen bond, or by burial deep within the protein. The similarity of the α- and β-subunits of Hb A often results in resonance overlap; this problem is reduced by recording separate spectra on chain-selectively isotopically labeled samples.[7] Using this technique, and earlier 1D ^{1}H NMR results, the side-chain ^{1}H and ^{15}N resonances of all 38 histidyl residues in HbCO A have been assigned.[44−46]

Parts of the echo anti-echo HMQC spectra of chain-selectively ^{15}N-labeled oxy- and carbonmonoxy-Hb A are shown superimposed in Figure 3. The spectra were acquired without ^{15}N decoupling; therefore, doublets are observed for directly bonded ^{15}N−^{1}H pairs. Most of the sharp cross-peaks with ^{1}H chemical shifts between 6.3 and 8.6 ppm originate from multiple-bond couplings within the solvent-exposed histidines of Hb A. There are no corresponding NH doublet cross-peaks for these histidines because of fast (submillisecond) exchange with water protons. However, doublets are seen at ($H\delta_1$, $N\delta_1$) of the proximal histidines α87His and β92His in both HbCO and HbO_2, as these protons are sufficiently protected that their exchange rate with solvent is much slower than the one-bond scalar coupling of ∼95 Hz. For the distal histidines α58His and β63His, the pattern of sharp cross-peaks indicates that these histidyl residues are neutral and adopt the $N\epsilon_2$ tautomerization state. In the spectrum of HbCO A, no doublet cross-peak characteristic of an NH moiety can be detected, presumably because of exchange with a water molecule in the distal heme pocket. On the other hand, in the spectrum of HbO_2 A, such doublets are clearly visible, indicating that the $H\epsilon_2$ proton is stabilized

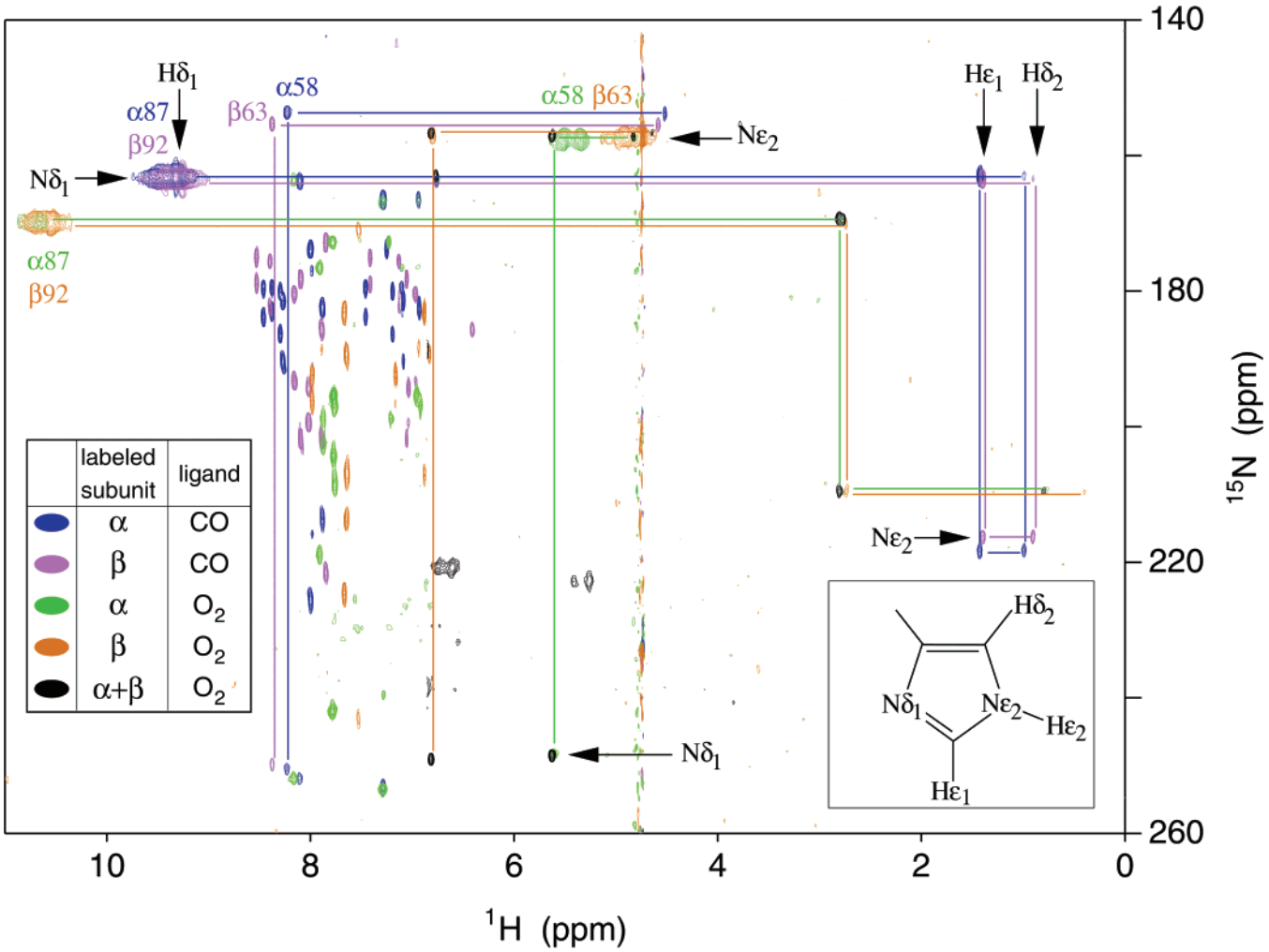

Figure 3. Histidine region of the 600-MHz (^{1}H, ^{15}N) echo anti-echo HMQC spectra of chain-selectively and fully ^{15}N-labeled HbCO A and HbO_2 A in water and D_2O at 29 °C. Cross-peaks in blue, violet, green, and orange come from spectra of ^{15}N-α-labeled HbCO A, ^{15}N-β-labeled HbCO A, ^{15}N-α-labeled HbO_2 A, and ^{15}N-β-labeled HbO_2 A, respectively. These experiments used a large spectral width in ^{15}N and a short refocusing delay (see ref 47 for experimental details). The spectra were acquired without ^{15}N decoupling; therefore, doublets are observed for directly bonded ^{15}N−^{1}H pairs. Also shown in green is a spectrum of ^{15}N-α-labeled HbO_2 A with a smaller ^{15}N spectral width and a longer refocusing delay, set in order to eliminate the α58His ($H\epsilon_2$, $N\epsilon_2$) doublet which overlaps the $H\epsilon_1$ cross-peak at 5.64 ppm. Cross-peaks in black are those of fully ^{15}N-labeled HbO_2 A in D_2O solution, which used a narrow ^{15}N spectral width and a short refocusing delay. Cross-peaks originating from the same residue are connected by lines. Other cross-peaks originate from the solvent-exposed and interfacial histidyl residues. Reproduced with permission from ref 47. Copyright 2000 National Academy of Sciences.

against exchange by a H-bond between the distal His and the O_2 ligand in both the α- and β-subunits. This finding[47] supports the hydrogen-bonding mechanism for the stabilization of O_2 versus CO binding in hemoglobin, in agreement with the growing consensus for myoglobin, as discussed above.

3.2. Cooperativity: Models and Mechanisms

Figure 4A shows the oxygen-binding curve of Hb A at different values of pH in the absence and presence of 2,3-bisphosphoglycerate (2,3-BPG) and inositol hexaphosphate (IHP). Here, the saturation Y (i.e., the fraction of oxygen-binding sites of Hb A that are liganded) is plotted versus pO_2, the partial pressure of oxygen in Torr (mm of Hg). The oxygen affinity of Hb is also affected by other intracellular solutes and ions such as CO_2 and Cl^- (results not shown). The sigmoidal shape of the binding curve suggests that the binding of O_2 to Hb A is cooperative, in that the binding of the first O_2 to a tetrameric hemoglobin molecule enhances the oxygen affinity of the remaining three unliganded subunits, the binding of the second O_2 to the same tetramer further increases the affinity of the remaining two unliganded subunits, and so on. This property of cooperativity allows Hb to load and release oxygen at appropriate oxygen pressures. Hb in red blood cells encounters a high oxygen pressure ($pO_2 = 100$ Torr) in the lungs, where it becomes approximately 95% saturated with oxygen. In the capillaries of tissues with moderate oxygen consumption, pO_2 will be 30−40 Torr, and each hemoglobin molecule will release approximately one or two molecules of oxygen. This makes the affinity of the remaining oxygens very sensitive to further decreases in oxygen pressure, so that these O_2 molecules are released relatively easily in rapidly metabolizing tissue, where pO_2 may be as low as 10−15 Torr.

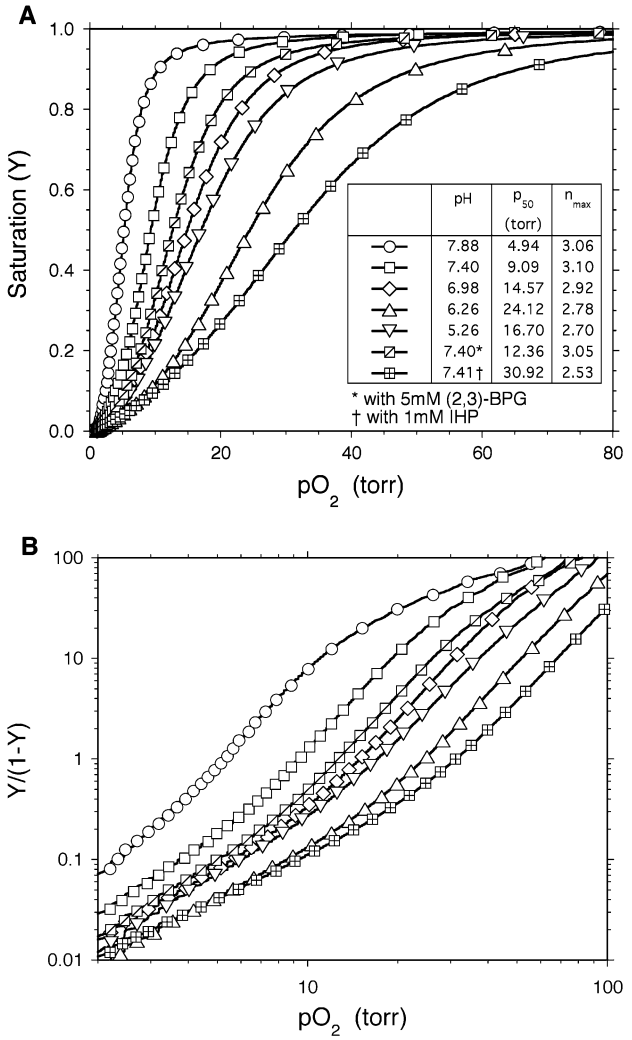

Figure 4. (A) Measured oxygen-binding curves of Hb A in 0.1 M phosphate buffer at 29 °C at several values of pH in the absence of allosteric effectors, at pH 7.40 in the presence of 5 mM 2,3-BPG, and at pH 7.41 in the presence of 1 mM IHP. The amount of oxygen bound to Hb is determined by monitoring the optical spectrum and comparing it to the characteristic spectra of the pure oxy and deoxy forms of the protein. The free O_2 concentration of the Hb sample is measured using an oxygen electrode. This measurement is made automatically as the Hb is continuously oxygenated (or deoxygenated) using a Hemox Analyzer (TCS Medical Products, Huntington Valley, PA). (B) Hill plots corresponding to the binding curves shown in part A.

The cooperative binding of oxygen by hemoglobin can be described by the Hill equation.[15] For a protein P which binds n oxygen molecules in an all-or-none manner, i.e., with perfect cooperativity, the binding reaction can be written

$$P + nO_2 \leftrightarrows P(O_2)_n.$$

For this reaction, the saturation is related to the ligand concentration by the Hill equation

$$\log\left(\frac{Y}{1-Y}\right) = n \log pO_2 - n \log p_{50} \qquad (1)$$

where p_{50} is a measure of the protein's oxygen affinity, defined as the value of pO_2 when half of the oxygen-binding sites are occupied. A low value of p_{50} corresponds to a high oxygen affinity. For this model of binding, a plot of $\log[Y/(1-Y)]$ versus $\log[pO_2]$, called a Hill plot, would be a straight line with a slope of n and an intercept on the $\log[pO_2]$ axis of $\log p_{50}$. However, the Hill plot observed for Hb A (shown in Figure 4B) exhibits a sigmoidal shape, indicating that binding occurs in stages, such that the oxygen affinity of the protein depends on the number of subunits in the tetramer that are already liganded. The asymptotic behavior of the oxygen-binding curve at very high and very low values of pO_2 indicates that the fourth oxygen molecule to bind to Hb A does so with ~100-fold higher affinity than the first. The Hill coefficient n_{max}, defined as the maximum slope along the Hill plot, indicates the degree of cooperativity of O_2 binding. For Hb A, n_{max} is approximately 3.0, suggesting the existence of partially oxygenated species, i.e., Hb tetramers with one, two, or three bound O_2 molecules.

The cooperativity of oxygen binding to hemoglobin implies communication between oxygen-binding sites, such that the ligation state of one heme affects the O_2-binding affinity of other hemes in the same tetramer. As the oxygen-binding sites are separated by large distances (in excess of 25 Å), any interactions between them must be mediated through the structure of the protein. On the basis of the crystal structures of Hb in the deoxy (T) and ligated (R) states, Perutz[17] proposed a stereochemical mechanism for the cooperative oxygenation of Hb. In deoxy-Hb, the heme porphyrins are domed, so that each iron atom is displaced approximately 0.6 Å out of the heme plane, toward the proximal His (F8). Upon ligation, the bonds between the iron and porphyrin nitrogens contract, so that the iron moves into the heme plane. To avoid a steric clash, the proximal histidine (F8) must tilt slightly, so that the F helix moves laterally approximately 1 Å across the heme (Figure 1D). According to Perutz's model, changes in tertiary structure propagate to the C-helix and the FG segment, which are involved in the $\alpha_1\beta_2$ subunit interfaces. Steric constraints prevent the subunit of Hb from adopting the tertiary structure of oxy-Hb while they remain in the quaternary arrangement of the T conformation. As successive oxygen molecules bind to T-state Hb, strain accumulates in the liganded subunits until the molecule snaps into the R conformation, undergoing a quaternary rearrangement at the switch region, as described above. It has been proposed that this quaternary shift must occur simultaneously at the $\alpha_1\beta_2$ and $\alpha_2\beta_1$ interface, because of the rigidity of the $\alpha_1\beta_1$ and $\alpha_2\beta_2$ interfaces.[48] A continuous transition from the T to the R quaternary structure is hindered by the stereochemistry of the switch region. The existence of two discrete, stable quaternary structures of Hb, as proposed by Perutz, is consistent with a two-state, concerted model of cooperativity. A key feature of the Perutz model for cooperativity is the coupling of the bond between the heme iron and the proximal histidyl residue to protein structural rearrangements.[17] An experimental test of the role of the proximal histidyl residues in the Perutz model for cooperative oxygen-

ation of Hb A has been reported.[49,50] In these studies, Ho and co-workers detached the bond between heme iron and the proximal histidyl residue by replacing the proximal histidine by a glycine. This detachment allows them to determine directly the contribution of proximal histidyl residue coupling to the cooperativity of ligand binding. The experimental results show that the proximal coupling mechanism as proposed by Perutz contributes approximately two-thirds of the total interaction energy between the hemes, the remaining third resulting from alternate coupling pathways.[49] In a further investigation of the distal ligand reactivity and quaternary structure, they have investigated three proximally detached rHbs, rHb (H87G), rHb (H92G), and rHb (H87G, H92G).[50] They have found that in the distally liganded Hb, the T-state is compatible with proximal linkages in the β-chains but not the α-chains. Comparing ligand association and dissociation rates between rHb (H87G) with the T- and R-states of Hb A indicates that, at the α-chains, CO affinity is modulated entirely by the proximal linkage, rather than by distal interactions. Some residual allosteric interactions remain at the β-chains of rHb (H87G).[49,50]

The concerted model proposed by Monod, Changeux, and Wyman[51] is based on the conservation of symmetry in an oligomeric protein at all stages of ligand binding. This model, called the MWC model, assumes that the protein interconverts between two conformations: a low-affinity T form and a high-affinity R form. All the subunits of a particular molecule must have the tertiary structure characteristic of one of these two forms; hybrids are disallowed. Thus, the transition from T to R is concerted in that all four subunits must change conformation in unison. The ligand-binding affinity of a subunit depends only on whether it is in the T or R state and is otherwise independent of whether neighboring subunits are liganded. In this model, the free energy of ligand binding stabilizes the R state relative to the T state. At all concentrations of ligand, an equilibrium exists between T- and R-state molecules. Binding of successive ligands increases the population of the high-affinity R-state molecules at the expense of T-state molecules, giving rise to positive cooperativity. The ligand saturation can be calculated in terms of three parameters: the normalized ligand concentration, the relative ligand-binding affinities of the T and R states, and the relative stabilities of the T and R states in the absence of ligand. These parameters can be adjusted to give an excellent fit of the MWC model to the measured oxygen-binding curve of Hb A.

In contrast to the MWC model, the sequential model of Koshland, Nemethy, and Filmer (the KNF model) allows subunits of different conformations to coexist within the same oligomeric protein molecule.[52] Each subunit is assumed to change its tertiary structure when it binds a ligand. This structural change alters the affinity of neighboring subunits through interactions at subunit interfaces. Thus, the deoxy to liganded transition occurs sequentially through a sequence of hybrids in response to tertiary structural changes induced by successive binding of ligands. The algebraic form of the fractional saturation depends on the specific model for interactions among subunits. Koshland and co-workers found that the best fit to observed binding data for Hb resulted from a square geometry model that assumes that stereochemical interaction occurs only between unlike subunits (α and β).[52] The KNF model is capable of providing an equally good fit as the MWC model to the measured oxygen-binding curve of Hb; therefore, such data alone cannot distinguish between the concerted and sequential mechanisms of cooperativity.

The question of whether the structural changes in Hb during oxygenation are concerted or sequential is the subject of ongoing controversy. In principle, this issue could be decided by determining the nature of the partially oxygenated species, as the sequential (KNF) model predicts that tetramers of Hb with one, two, or three bound O_2 molecules could contain subunits of mixed tertiary structure, while the concerted (MWC) model only allows a statistical ensemble of pure R-state or T-state tetramers. In practice, however, these ligation intermediates are extremely difficult to study, because the high cooperativity of hemoglobin suppresses their populations, in favor of the deoxy and fully ligated end-states. Also, individual partially ligated tetramers are highly labile, due to ligand mobility and dimer exchange. One way of generating large populations of intermediate ligated states is to subject HbCO to photolysis. A set of precise time-resolved optical spectra acquired following varying degrees of photolysis of HbCO A has been analyzed by Eaton and co-workers.[53] A very good fit of the kinetics data, as well as equilibrium data on ligand binding, was obtained using a concerted MWC model, extended to take into account geminate ligand rebinding and tertiary relaxation within the R quaternary structure. These modifications do not affect the fundamental postulate of the MWC model, that ligand binding within each quaternary structure is noncooperative.

Another means of studying ligation intermediates uses tightly bound oxygenation analogues to model the native O_2-ligated Hb subunits, and metal-substituted hemes incapable of binding O_2 to mimic the stereochemistry of natural deoxy Hb subunits. In particular, the $Fe^{2+}O_2$ subunits have been modeled by $Fe^{2+}CO$, Mn^{3+}, and $Fe^{3+}CN$ (termed CNmet), while deoxy subunits have been mimicked by Co^{2+}- and Zn^{2+}-substituted hemes. Using these stable analogues of oxy- and deoxy-subunits, model tetramers can be prepared which represent 4 of the 10 distinct tetrameric microstate species, i.e., fully ligated or unligated, both α-subunits ligated, or both β-subunits ligated. When these parent tetramers are mixed, they dissociate into dimers, which subsequently associate into hybrid tetramers including the singly and triply ligated, and asymmetric doubly liganded, tetramers, which represent the remaining six microstates.

Using techniques including cryogenic isoelectric focusing,[54] Ackers and co-workers have measured the abundance of each partially ligated species in equilibrium mixtures. Thermodynamic linkage relationships between the free energies of tetramer assembly and those of ligand binding are then used to derive

the free energies of cooperativity for each of the tetrameric species (see ref 55 and references therein). From data on several partially ligated model systems, a consensus distribution was seen, where both distinct triply ligated species had approximately the same cooperative free energy as the three doubly ligated tetramers having one ligated subunit on each of the $\alpha\beta$ dimers. Remarkably, however, the doubly ligated species with both ligands on the same dimer (i.e., $\alpha_1\beta_1$ or $\alpha_2\beta_2$) showed distinctly greater stability. This observation, together with studies of rHbs with mutations in the $\alpha_1\beta_2$ subunit interface, led to the formulation of a symmetry rule or molecular code mechanism. Under this mechanism, the T → R quaternary transition is triggered whenever heme-site binding creates a tetramer with at least one ligated subunit on each dimeric half-molecule ($\alpha_1\beta_1$ or $\alpha_2\beta_2$).[56] The binding of the first ligand to deoxy-Hb creates a change in tertiary structure throughout the ligated dimer, which creates strain at the T ($\alpha_1\beta_2$ or $\alpha_2\beta_1$) interface, manifested as an unfavorable free energy penalty. The binding of a second ligand to the other subunit within the same dimer creates a smaller penalty, resulting in cooperativity within the dimer, which is present only when the dimer is part of a tetramer; binding to a free $\alpha\beta$ dimer is noncooperative. Upon ligation of the second dimer, the accumulated free energy penalty is sufficient to drive the interdimer contacts to rearrange from the T to the R conformation, in a concerted fashion. Thus, the symmetry rule model incorporates elements of both the sequential and concerted models, as the cooperativity resulting from intersubunit communication within each half-tetramer is coupled to the global T → R quaternary transition.

This model of hemoglobin cooperativity has been questioned by Shibayama and co-workers,[57,58] who found that significant valency exchange (i.e., electron transfer between iron atoms, enabling the rearrangement of CN^-) occurs in mixtures of deoxy and cyanomet-Hb A over long periods of anaerobic incubation. This effect can lead to the overestimation of the free energy of dimer−tetramer assembly of the $(\alpha\beta)(\alpha^{+CN-}\beta^{+CN-})$ species, which is a key piece of evidence in favor of the symmetry rule model. Shibayama has also presented evidence, obtained from studies of Ni^{2+}/Fe^{2+}−CO hybrid tetramers stabilized by encapsulation in silica gels, that two conformations of widely different binding affinity coexist in each doubly liganded hemoglobin.[59] These results, as well as a direct O_2-binding investigation of Zn^{2+}/Fe^{2+} hybrids,[60] provide support for the traditional MWC model. However, Ackers et al.[61] have asserted that the cooperative free energy of the $(\alpha\beta)(\alpha^{+CN-}\beta^{+CN})$ species remains uniquely stable after correcting for the effects of valency exchange, so the symmetry rule retains its validity. In a recent study[62] of tetramers containing a single modified residue in only one of the four subunits, Ackers and co-workers have concluded that the removal of interdimer contacts weakens the T ($\alpha_1\beta_2$ or $\alpha_2\beta_1$) interface but is not communicated from heme to heme across that interface. Rather, modification of a residue in a single subunit affects the affinity of the complementary subunit within the same dimer. These results are consistent with the intradimer cooperativity of the symmetry rule model.

3.3. Heterotropic Allosteric Effectors and the Bohr Effect

The cooperative oxygenation of hemoglobin is an example of a homotropic allosteric effect, wherein the binding of a ligand to a particular site affects the affinity of a separate, often distant, binding site for the same type of ligand. The oxygen binding of hemoglobin is also modulated by heterotropic allosteric effectors including hydrogen and chloride ions, carbon dioxide, phosphate, 2,3-BPG, and IHP, which bind to sites distinct from the oxygen-binding sites.[1] These molecules do not affect the binding of O_2 to Mb; their effects on hemoglobin depend on the protein's oligomeric nature. Allosteric effectors allow Hb to take up and release oxygen in response to changing physiological conditions. An important example is 2,3-BPG, a polyanion which binds to residues His2, Lys82, and His146 of both β-chains of Hb A, effectively propping these chains apart, across the central cavity of the tetramer.[63] The central cavity of oxy-Hb A is too narrow to accommodate the 2,3-BPG molecule; however, this allosteric effector binds favorably to the protein in the deoxy (T) conformation, where the cavity is wider. Thus, 2,3-BPG lowers the oxygen affinity of Hb A by shifting the T ↔ R equilibrium toward the T state. In the absence of 2,3-BPG, Hb A would give up much less oxygen when passing through the capillaries. When individuals adjust to life at a high altitude, where oxygen is less plentiful, the concentration of 2,3-BPG increases in their red blood cells, allowing more oxygen to be released to the tissues.[15]

Another heterotropic allosteric effector of physiological importance is H^+; i.e., the oxygen affinity of Hb A depends on pH. At pH values above 6.5, an increase in pH shifts the oxygen-binding curves to the left, as shown in Figure 4. Thus, a lower partial pressure of oxygen (p_{50}) is sufficient to induce 50% saturation of O_2-binding sites, corresponding to an increase in oxygen affinity. This pH dependence, known as the alkaline Bohr effect, implies a higher H^+-binding affinity for deoxy-Hb than oxy-Hb, so that oxygenation results in the release of protons. The alkaline Bohr effect facilitates the exchange of oxygen and carbon dioxide. As blood circulates through the capillaries, CO_2 enters the red blood cells, where carbonic anhydrase catalyzes the reaction $CO_2 + H_2O \leftrightarrows HCO_3^- + H^+$. The resulting protons are taken up by Hb, which, in accordance with the alkaline Bohr effect, is induced to release oxygen. As bicarbonate ions diffuse through the erythrocyte membrane into the surrounding plasma, charge neutrality is maintained by the diffusion of chloride into the cell.[15] Chloride binds to deoxy-Hb A, between the amino-terminal group of each α-chain and the guanidino-group of the other α-chain's carboxy-terminal arginine. Thus, the α-subunits of deoxy-Hb A are linked by Cl^- in a head-to-tail manner. This chloride binding stabilizes the protonation of the N-terminal amino group, thereby increasing its p*K*. On oxygenation,

both the Cl^- and the H^+ are released. Thus, the Bohr effect is linked to chloride-binding. A small portion of CO_2 also binds reversibly to the N-terminal amino groups of Hb, in a reaction that liberates additional protons. The resulting carbamino-Hb has a lower oxygen affinity than hemoglobin in the absence of CO_2. The interplay between the binding of oxygen and the heterotropic allosteric effectors CO_2, Cl^-, and H^+ allows hemoglobin to take up and release oxygen and carbon dioxide reciprocally, both in the lungs and capillaries, and to deliver additional oxygen to highly active muscles as they generate lactic and carbonic acid.

At values of pH below 6.5, ligated Hb has a higher affinity for H^+ ions than does deoxy-Hb. In this regime, the acid Bohr effect holds, where oxygen affinity increases with decreasing pH, and the Hb molecule takes up protons upon oxygenation. Both the acid and alkaline Bohr effects arise from changes in the local environments of amino acid residues, which accompany the T → R conformational change in hemoglobin, and alter the p*K* values of these residues. Groups which contribute to the Bohr effect include the imidazoles of surface histidyl residues, the amino-termini of the α- and *β*-chains, and possibly other proton binding sites whose p*K* values have been significantly shifted into the physiological pH range because of unique structural and conformational arrangements in the Hb molecule.[64] The Bohr effect can be determined from the change in oxygen affinity as a function of pH. According to Wyman's linkage model,[65,66] there is an exact relationship between the change of oxygen affinity and the number of H^+ ions released or taken up as a function of pH. The net Bohr effect is the sum of contributions from each amino acid residue that has a p*K* value in the deoxy form differing from that in the oxy (or CO) form of hemoglobin. The Bohr effect contribution of each residue, in terms of the number of protons released per Hb tetramer upon the transition from T to R, is given by[45,46]

$$\Delta\nu_{\mathrm{H}}(i) = 2\left(\frac{K_i^{\mathrm{R}}}{[\mathrm{H}^+] + K_i^{\mathrm{R}}} - \frac{K_i^{\mathrm{T}}}{[\mathrm{H}^+] + K_i^{\mathrm{T}}}\right) \qquad (2)$$

where K_i is the proton dissociation constant of the residue, and superscripts R and T denote the oxy- (or carbonmonoxy-) and deoxy-forms of the protein.

Equation 2 shows that the contribution of each histidyl to the Bohr effect can be calculated from the change in its p*K* value on binding oxygen (or carbon monoxide) to deoxy-Hb A. As noted above (section 3.1), NMR spectroscopy is very well suited for studying histidyl residues because the C2 ($H\epsilon_1$) proton resonances are usually resolved from other proton resonances. Any degeneracy of the C2 ^1H resonances of different histidyls can usually be resolved by a 2D HMQC spectrum of ^{15}N-labeled Hb, which provides a pattern of cross-peaks that characterizes the tautomeric state of each histidyl. The C2 resonances of all 38 histidyls in both deoxy- and carbonmonoxy-Hb A have been assigned by 1D and 2D NMR studies of Hb A as well as mutant and chemically modified Hbs.[7,44−46] Accurate p*K* values are determined by a nonlinear least-squares fit of the chemical shift *δ* of each C2 proton as a function of pH to the equation[44]

$$\delta = \frac{\delta^+[\mathrm{H}^+]^n + \delta^0[K]^n}{[\mathrm{H}^+]^n + [K]^n} \qquad (3)$$

where δ^+ and δ^0 are the chemical shifts in the protonated and unprotonated forms of the histidyl residue, respectively, *K* is the H^+ dissociation constant of the residue, and *n* is the titration coefficient. Note that although *n* is often called the Hill coefficient for the proton titration of the histidyl residue, it should not be confused with the Hill coefficient for oxygen binding, which characterizes the cooperativity of hemoglobin. Fitted values of *n* substantially smaller than 1.0, as seen for *β*146 in HbCO A, indicate that interactions with another ionizing group(s) are taking place.[44] The p*K* values of all surface histidines of Hb A in deoxy and CO-ligated forms are listed in Table 1; see ref 46 for additional details.

Table 1. p*K* Values of Histidyl Residues in Deoxy-Hb A and HbCO A in 0.1 M HEPES Plus 0.1 M Chloride in D_2O at 29 °C from a Nonlinear Least-Squares Fit of Experimental Data to Equation 3[a]

site	p*K* (CO)	p*K* (deoxy)
α20	7.08 ± 0.01	7.02 ± 0.01
α45	6.12 ± 0.02	5.25 ± 0.15
α50	6.90 ± 0.02	7.14 ± 0.01
α72	7.27 ± 0.01	7.47 ± 0.01
α89	6.25 ± 0.03	6.80 ± 0.01
α112	7.53 ± 0.01	7.49 ± 0.01
*β*2	6.39 ± 0.01	6.17 ± 0.02
*β*77	7.79 ± 0.01	7.46 ± 0.01
*β*97	7.75 ± 0.02	8.01 ± 0.01
*β*116	6.13 ± 0.05	6.35 ± 0.04
*β*117	6.39 ± 0.02	6.43 ± 0.07
*β*143	5.57 ± 0.06	4.70 ± 0.05
*β*146	6.42 ± 0.03	7.93 ± 0.02

[a] Values are reproduced from Table 2 of ref 46 except for the p*K* of α45His in deoxy Hb A (V. Simplaceanu and C. Ho, unpublished results). Because of very low p*K* value for α45His, there were difficulties in determining this value accurately.

Using the fitted p*K* values and eq 2, we can find the contribution of each histidyl to the Bohr effect, in terms of the number of H^+ ions released per Hb tetramer upon oxygenation (Figure 5). From this figure, it is clear that several histidyl residues contribute to the Bohr effect, and some oppose the net Bohr effect. The largest contribution to the alkaline Bohr effect is that of *β*146His, while *β*143His and α45His make the largest contributions to the acid Bohr effect. The sum of the contributions from the 26 surface histidyl residues (13 per α*β* dimer) agrees very well with the measured net acid Bohr effect of Hb A but does not completely account for the measured alkaline Bohr effect. The discrepancy may be due to the contribution of other groups, including the amino-termini,[67] which are not taken into account in Figure 5. The addition of anions has been shown to diminish or reverse the contribution of specific histidyl residues to the overall Bohr effect.[45,68] Thus, the Bohr effect depends on the intricate arrangement and interactions of all hydrogen and anion binding sites in the Hb molecule. It is an example of a global network of electrostatic

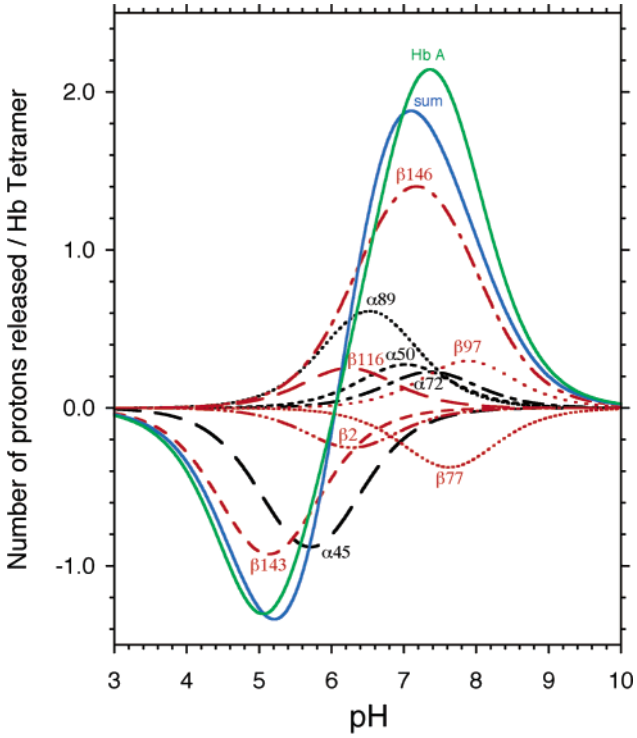

Figure 5. Bohr effect of Hb A in D_2O in 0.1 M HEPES buffer plus 0.1 M NaCl at 29 °C. The net Bohr effect of Hb A (green) is determined from oxygen dissociation studies. The contributions of individual histidyl residues are calculated using p*K* values measured by NMR techniques.[46] The contributions of α20His, α112His, and *β*117His are negligible and are not shown. Sum (blue) is the summation of the contribution of all 26 surface histidyl residues.

interactions, rather than a few specific amino acid residues, playing a dominant role in an important physiological function.

4. Solution Conformation, Dynamics, and Intersubunit Communication

The traditional two-state description of Hb, where the T and R states are implicitly identified with the X-ray crystal structures of deoxy- and liganded-Hb, has been complicated by the discovery of a second, distinctly different structure of the liganded protein, called R2. This finding raises the question of which crystal structure, R, R2, or a mixture of both, represents the structure of liganded Hb A in solution under physiological conditions. The observation that cooperativity and allosteric effects are absent in the crystalline state[69] provides further motivation for studying hemoglobin in the solution state, where it performs its physiological functions. The individual subunits, as well as the $\alpha_1\beta_1$ and $\alpha_2\beta_2$ subunit interfaces, are stabilized by a large number of close contacts and hydrogen bonds, and are essentially identical in the R and R2 X-ray structures.[18] These structures differ mainly in the relative position and orientation of the $\alpha_1\beta_1$ and $\alpha_2\beta_2$ dimers. Similarly, the $\alpha\beta$ dimers of Hb A in solution are likely to closely resemble their X-ray crystal structures.

The relative orientation of protein domains or subunits of known structure can be determined by recently developed NMR methodology in which the protein is weakly aligned with respect to the static magnetic field.[70,71] Such alignment is achieved by dissolving the protein in a liquid crystalline medium, which, in the presence of a strong magnetic field, provides a distribution of boundaries with a preferred orientation. The aligned medium breaks the isotropic symmetry of the protein's tumbling in solution and (provided the protein is ^{15}N-labeled) induces a residual dipolar coupling (RDC) at each amide (^1H, ^{15}N) group. The value of each RDC depends on the polar angles of the corresponding NH bond vector with respect to the alignment coordinate frame. Thus, the set of observed RDCs imposes orientational constraints on rigid substructures of the protein.

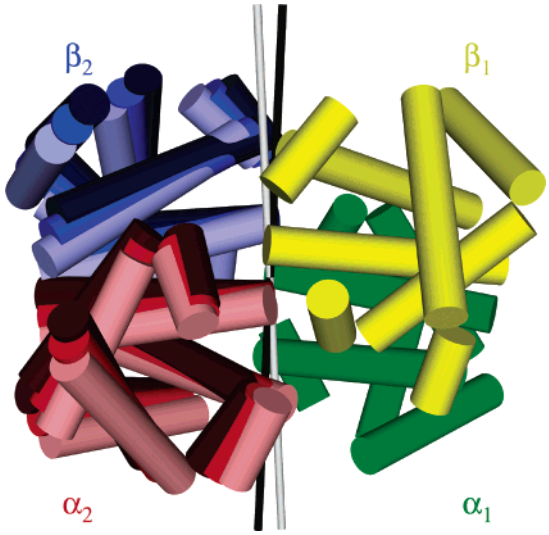

Figure 6. Schematic illustration of the R and R2 crystal structures, together with the solution conformation, of HbCO A. Helices are shown as cylinders. Here, the $\alpha_1\beta_1$ dimers of the two structures have been superimposed and are indistinguishable. The α_2- and β_2-subunits of the R, solution, and R2 structures are shown in dark, medium, and light shades (respectively) of red and blue. The C_2 symmetry axes of the R and R2 structures are shown as thin black and white rods, respectively. Reproduced with permission from ref 74. Copyright 2003 National Academy of Sciences.

Two different liquid crystalline media, filamentous bacteriophage Pf1[72] and phospholipid bicelles,[73] were found to align HbCO A along distinct directions. For both media, the RDCs were measured as differences between $^1H-^{15}N$ couplings in the presence and absence of the aligning medium. The $\alpha\beta$ dimers were modeled as rigid bodies and allowed to rotate (while preserving the C_2 symmetry of the tetramer) so as to optimize the fit between observed and predicted RDCs.[74] The optimal quaternary structure was found to lie exactly halfway between the R and R2 X-ray structures, as shown in Figure 6. This finding is consistent with either a static structure, or a dynamic average over an ensemble which includes the R and R2 structures. The latter possibility is indicated by ^{15}N relaxation rates (unpublished results), which reveal significant conformational exchange contributions at contact sites between the $\alpha\beta$ dimers, particularly $\alpha_1$94Asp and $\beta_2$37Trp, which form the flexible joint of the $\alpha_1\beta_2$ interface. The existence of a rapid equilibrium among multiple solution conformations is consistent with the conclusion of Arnone and

co-workers,[21] on the basis of the crystallization of bovine HbCO with structures intermediate between R and R2, that the $\alpha_1\beta_2$ interface of liganded Hb has a range of energetically accessible structures, which are related to each other by a simple sliding motion. The structural differences are very slight in terms of the number and strength of intersubunit contacts and are therefore likely to involve only small free energy differences. The crystallization (under moderately different conditions) of liganded Hb in R, R2, and intermediate forms suggests that a family of conformers coexist in solution, and that the process of crystallization will select (or purify) the particular structure which corresponds to a free energy minimum, under the crystallization conditions used.[21] While X-ray crystallography provides a detailed characterization of each such crystal structure, solution NMR can provide information on the dynamical ensemble of structures that occur under physiological conditions. These results highlight the complementarity of the X-ray crystallography and solution NMR approaches to elucidating the structure−function relationships of large multimeric proteins such as Hb.

Recent NMR studies using relaxation and proton exchange measurements have clearly shown that a number of amino acid residues in the $\alpha_1\beta_1$ interface (such α103His and α122His)[14,75] as well as in the $\alpha_1\beta_2$ interface (such as β37Trp)[76,77] have substantial flexibility/mobility in deoxy and/or ligated states. Even though the X-ray crystallographic results have suggested that the $\alpha_1\beta_1$ and the symmetry-related $\alpha_2\beta_2$ interfaces undergo very little structural changes in the cooperative oxygenation process,[1,16] several studies suggest that the interactions with this subunit interface are coupled to allostery. For the $N\epsilon_2H$ protons of 103His and 122His that form intersubunit H-bonds with β131Gln and β35Tyr, respectively,[14] exchange rates with solvent are found to be significantly faster in the T state than in the R state and also depend on the nature of the buffer, suggesting that the strength of these H-bonds changes as a result of the quaternary structure transition, increasing in strength in the R-quaternary structure.[14,75] Similar conclusions have also been reached in a mutagenesis study that targeted the intersubunit H-bond acceptor of α103His, i.e., β131Gln.[14] We have found that substitution of β131Gln can affect the chemical environment of the $N\epsilon_2$Hs of both α103His and α122His, increasing the exchange rates of both $N\epsilon_2$Hs in the ligated form, and decreasing the oxygen affinity.[14] In addition, these amino acid substitutions also increase the rate of chemical modification of β93Cys, a residue near the proximal heme pocket that makes contacts in the $\alpha_1\beta_2$ subunit interface, suggesting that these $\alpha_1\beta_1$ intersubunit interactions may be coupled to the $\alpha_1\beta_2$ subunit interface, as well as to the distal ligand binding.[14] Our results on the sensitivity of the proton resonances at the $\alpha_1\beta_1$ subunit interface to distal ligand binding are consistent with the results reported by Ackers et al.[62]

5. Conclusions

The experimental results obtained from our recent NMR studies of isotopically labeled recombinant hemoglobins as summarized in this article have provided new insights into the structure−function relationship of hemoglobin in solution at atomic resolution. We would like to summarize our findings as follows: (i) With the accurately measured and assigned individual p*K* values for all surface histidyl residues of Hb A in both deoxy and CO forms, our results show that the Bohr effect of hemoglobin is not due to a few amino acid residues as first suggested from the crystal structures of hemoglobin.[17,48] In fact, a global network of electrostatic interactions plays a dominant role in the Bohr effect of hemoglobin. (ii) NMR reveals H-bonds between oxygen ligands and distal histidyl residues of both α- and β-chains of oxyhemoglobin, but no such H-bonds between carbon monoxide ligands and distal histidyl residues of carbonmonoxyhemoglobin. This finding provides a direct structural basis for the enhanced affinity of oxygen relative to carbon monoxide in hemoglobin as compared with free hemes. (iii) The solution structure of carbonmonoxyhemoglobin is neither the classical R structure (derived from high-salt crystals) nor the R2 structure (derived from low-salt crystals) on the basis of crystallographic structural determinations. The solution structure of HbCO A is a dynamic intermediate between the two previously solved R and R2 crystal structures. The fact that there is not a fixed R-structure, but a dynamic ensemble, raises a serious challenge to the classic switch mechanism of the stereochemical model for the cooperative oxygenation of hemoglobin as proposed by Perutz in 1970, namely the T → R transition. It should be mentioned that the structural and functional properties of Hb A inside red blood cells are essentially the same as those in solution as revealed by ^{1}H NMR studies.[78,79]

The results presented in this article illustrate the complementarity of the X-ray crystallography and solution NMR approaches to elucidating the structure−function relationships of large multimeric proteins such as Hb. Solution NMR techniques can provide detailed information regarding the conformations and interactions of specific amino acid residues in hemoglobin not seen by X-ray crystallography on Hb crystals. The NMR results show that hemoglobin is a rather flexible or adaptable molecule whose conformation can be adjusted in response to various perturbations, e.g., amino acid substitutions, binding of ligands, and/or allosteric effectors. It appears that allosteric interactions have multiple pathways for signal transmission in allosteric proteins.

6. Acknowledgments

We wish to thank our colleagues, Virgil Simplaceanu, Yue Yuan, and Nancy T. Ho, for helpful discussions and for providing unpublished data for this article. Our hemoglobin research is supported by research grants from the National Institutes of Health (R01HL-24525, P01HL-71064, and S10RR-11248).

7. References

(1) Dickerson, R. E.; Geiss, I. *Hemoglobin: Structure, Function, Evolution, and Pathology*; Benjamin/Cummings: Menlo Park, CA, 1983.

(2) Ho, C. *Adv. Protein Chem*. **1992**, *43*, 153.
(3) Ho, C.; Lukin, J. A. In *Encyclopedia of Life Sciences*; Nature Publishing Group: London, 2000.
(4) Ho, C. In *Encyclopedia of Magnetic Resonance*; Grant, D. M., Harris, R. K., Eds.; John Wiley & Sons, Ltd.: Sussex, U.K., 1995; Vol. 4.
(5) Ho, C.; Perussi, J. R. *Methods Enzymol*. **1994**, *232* (Part C), 97.
(6) Shen, T. J.; Ho, N. T.; Simplaceanu, V.; Zou, M.; Green, B. N.; Tam, M. F.; Ho, C. *Proc. Natl. Acad. Sci. U.S.A*. **1993**, *90*, 8108.
(7) Simplaceanu, V.; Lukin, J. A.; Fang, T. Y.; Zou, M.; Ho, N. T.; Ho, C. *Biophys. J*. **2000**, *79*, 1146.
(8) Kim, H. W.; Shen, T. J.; Sun, D. P.; Ho, N. T.; Madrid, M.; Tam, M. F.; Zou, M.; Cottam, P. F.; Ho, C. *Proc. Natl. Acad. Sci. U.S.A*. **1994**, *91*, 11547.
(9) Kim, H. W.; Shen, T. J.; Sun, D. P.; Ho, N. T.; Madrid, M.; Ho, C. *J. Mol. Biol*. **1995**, *248*, 867.
(10) Tsai, C. H.; Shen, T. J.; Ho, N. T.; Ho, C. *Biochemistry* **1999**, *38*, 8751.
(11) Fang, T. Y.; Simplaceanu, V.; Tsai, C. H.; Ho, N. T.; Ho, C. *Biochemistry* **2000**, *39*, 13708.
(12) Tsai, C. H.; Larson, S. C.; Shen, T. J.; Ho, N. T.; Fisher, G. W.; Tam, M. F.; Ho, C. *Biochemistry* **2001**, *40*, 12169.
(13) Cheng, Y.; Shen, T. J.; Simplaceanu, V.; Ho, C. *Biochemistry* **2002**, *41*, 11901.
(14) Chang, C. K.; Simplaceanu, V.; Ho, C. *Biochemistry* **2002**, *41*, 5644.
(15) Voet, D.; Voet, J. G. *Biochemistry*, 2nd ed.; John Wiley & Sons: New York, 1995.
(16) Baldwin, J.; Chothia, C. *J. Mol. Biol*. **1979**, *129*, 175.
(17) Perutz, M. F. *Nature* **1970**, *228*, 726.
(18) Silva, M. M.; Rogers, P. H.; Arnone, A. *J. Biol. Chem*. **1992**, *267*, 17248.
(19) Smith, F. R.; Simmons, K. C. *Proteins: Struct., Funct., Genet*. **1994**, *18*, 295.
(20) Srinivasan, R.; Rose, G. D. *Proc. Natl. Acad. Sci. U.S.A*. **1994**, *91*, 11113.
(21) Mueser, T. C.; Rogers, P. H.; Arnone, A. *Biochemistry* **2000**, *39*, 15353.
(22) Tame, J. R. *Trends Biochem. Sci*. **1999**, *24*, 372.
(23) Fermi, G.; Perutz, M. F.; Shaanan, B.; Fourme, R. *J. Mol. Biol*. **1984**, *175*, 159.
(24) Shaanan, B. *J. Mol. Biol*. **1983**, *171*, 31.
(25) Olson, J. S.; Phillips, G. N. *J. Biol. Inorg. Chem*. **1997**, *2*, 5544.
(26) Collman, J. P.; Brauman, J. I.; Halbert, T. R.; Suslick, K. S. *Proc. Natl. Acad. Sci. U.S.A*. **1976**, *73*, 3333.
(27) Springer, B. A.; Sligar, S. G.; Olson, J. S.; Phillips, G. N. *Chem. Rev*. **1994**, *94*, 699.
(28) Li, X.-Y.; Spiro, T. G. *J. Am. Chem. Soc*. **1988**, *110*, 6024.
(29) Ray, G. B.; Li, X.-Y.; Ibers, J. A.; Sessler, J. L.; Spiro, T. G. *J. Am. Chem. Soc*. **1994**, *116*, 162.
(30) Spiro, T. G.; Kozlowski, P. M. *Acc. Chem. Res*. **2001**, *34*, 137.
(31) Kachalova, G. S.; Popov, A. N.; Bartunik, H. D. *Science* **1999**, *284*, 473.
(32) Vojtechovsky, J.; Chu, K.; Berendzen, J.; Sweet, R. M.; Schlichting, I. *Biophys. J*. **1999**, *77*, 2153.
(33) Stec, B.; Phillips, G. N. *Acta Crystallogr., Sect. D: Biol. Crystallogr*. **2001**, *57*, 751.
(34) Lim, M.; Jackson, T. A.; Anfinrud, P. A. *Science* **1995**, *269*, 962.
(35) McMahon, M. T.; deDios, A. C.; Godbout, N.; Salzmann, R.; Laws, D. D.; Le, H. B.; Havlin, R. H.; Oldfield, E. *J. Am. Chem. Soc*. **1998**, *120*, 4784.
(36) Spiro, T. G.; Kozlowski, P. M. *J. Am. Chem. Soc*. **1998**, *120*, 4524.
(37) Sage, J. T. *J. Biol. Inorg. Chem*. **1997**, *2*, 5537.
(38) Unno, M.; Christian, J. F.; Olson, J. S.; Sage, J. T.; Champion, P. M. *J. Am. Chem. Soc*. **1998**, *120*, 2670.
(39) Phillips, S. E. V.; Schoenborn, B. P. *Nature* **1981**, *292*, 81.
(40) Markley, J. L.; Kainosho, M. In *NMR of Macromolecules: A Practical Approach*; Roberts, G. C. K., Ed.; Oxford University Press: Oxford, 1993.
(41) Pelton, J. G.; Torchia, D. A.; Meadow, N. D.; Roseman, S. *Protein Sci*. **1993**, *2*, 543.
(42) Stockman, B. J.; Reily, M. D.; Westler, W. M.; Ulrich, E. L.; Markley, J. L. *Biochemistry* **1989**, *28*, 230.
(43) Oh, B. H.; Mooberry, E. S.; Markley, J. L. *Biochemistry* **1990**, *29*, 4004.
(44) Busch, M. R.; Mace, J. E.; Ho, N. T.; Ho, C. *Biochemistry* **1991**, *30*, 1865.
(45) Sun, D. P.; Zou, M.; Ho, N. T.; Ho, C. *Biochemistry* **1997**, *36*, 6663.
(46) Fang, T. Y.; Zou, M.; Simplaceanu, V.; Ho, N. T.; Ho, C. *Biochemistry* **1999**, *38*, 13423.
(47) Lukin, J. A.; Simplaceanu, V.; Zou, M.; Ho, N. T.; Ho, C. *Proc. Natl. Acad. Sci. U.S.A*. **2000**, *97*, 10354.
(48) Perutz, M. F.; Wilkinson, A. J.; Paoli, M.; Dodson, G. G. *Annu. Rev. Biophys. Biomol. Struct*. **1998**, *27*, 1.
(49) Barrick, D.; Ho, N. T.; Simplaceanu, V.; Dahllquist, F. W.; Ho, C. *Nat. Struct. Biol*. **1997**, *4*, 78.
(50) Barrick, D.; Ho, N. T.; Simplaceanu, V.; Ho, C. *Biochemistry* **2001**, *40*, 3780.
(51) Monod, J.; Wyman, J.; Changeux, J. P. *J. Mol. Biol*. **1965**, *12*, 88.
(52) Koshland, D. E., Jr.; Nemethy, G.; Filmer, D. *Biochemistry* **1966**, *5*, 365.
(53) Henry, E. R.; Jones, C. M.; Hofrichter, J.; Eaton, W. A. *Biochemistry* **1997**, *36*, 6511.
(54) Perrella, M.; Benazzi, L.; Shea, M. A.; Ackers, G. K. *Biophys. Chem*. **1990**, *35*, 97.
(55) Ackers, G. K. *Adv. Protein Chem*. **1998**, *51*, 185.
(56) Ackers, G. K.; Doyle, M. L.; Myers, D.; Daugherty, M. A. *Science* **1992**, *255*, 54.
(57) Shibayama, N.; Morimoto, H.; Saigo, S. *Biochemistry* **1997**, *36*, 4375.
(58) Shibayama, N.; Morimoto, H.; Saigo, S. *Biochemistry* **1998**, *37*, 6221.
(59) Shibayama, N. *J. Mol. Biol*. **1999**, *285*, 1383.
(60) Yun, K. M.; Morimoto, H.; Shibayama, N. *J. Biol. Chem*. **2002**, *277*, 1878.
(61) Ackers, G. K.; Holt, J. M.; Huang, Y.; Grinkova, Y.; Klinger, A. L.; Denisov, I. *Proteins* **2000**, *4* (Suppl), 23.
(62) Ackers, G. K.; Dalessio, P. M.; Lew, G. H.; Daugherty, M. A.; Holt, J. M. *Proc. Natl. Acad. Sci. U.S.A*. **2002**, *99*, 9777.
(63) Arnone, A. *Nature* **1972**, *237*, 146.
(64) Rao, M. J.; Acharya, A. S. *Biochemistry* **1992**, *31*, 7231.
(65) Wyman, J. *Adv. Protein Chem*. **1964**, *19*, 223.
(66) Wyman, J. *Adv. Protein Chem*. **1948**, *4*, 407.
(67) Kilmartin, J. V.; Rossibernardi, L. *Nature* **1969**, *222*, 1243.
(68) Busch, M. R.; Ho, C. E. *Biophys. Chem*. **1990**, *37*, 313.
(69) Eaton, W. A.; Henry, E. R.; Hofrichter, J.; Mozzarelli, A. *Nat. Struct. Biol*. **1999**, *6*, 351.
(70) Prestegard, J. H.; al-Hashimi, H. M.; Tolman, J. R. *Q. Rev. Biophys*. **2000**, *33*, 371.
(71) Tjandra, N.; Bax, A. *Science* **1997**, *278*, 1697.
(72) Hansen, M. R.; Mueller, L.; Pardi, A. *Nat. Struct. Biol*. **1998**, *5*, 1065.
(73) Sanders, C. R., II; Schwonek, J. P. *Biochemistry* **1992**, *31*, 8898.
(74) Lukin, J. A.; Kontaxis, G.; Simplaceanu, V.; Yuan, Y.; Bax, A.; Ho, C. *Proc. Natl. Acad. Sci. U.S.A*. **2003**, *100*, 517.
(75) Mihailescu, M.-R.; Russu, I. M. *Proc. Natl. Acad. Sci. U.S.A*. **2002**, *98*, 3773.
(76) Mihailescu, M.-R., Fronticelli, C.; Russu, I. M. *Proteins: Struct., Funct., Genet*. **2001**, *44*, 73.
(77) Yuan, Y.; Simplaceanu, V.; Lukin, J. A.; Ho, C. *J. Mol. Biol*. **2002**, *321*, 863.
(78) Fetler, B. K.; Simplaceanu, V.; VanderVen, N. S.; Lowe, I. J.; Ho, C. *J. Magn. Reson*. **1993**, *B101*, 17.
(79) Fetler, B. K.; Simplaceanu, V.; Ho, C. *Biophys. J*. **1995**, *68*, 681.
(80) Koradi, R.; Billeter, M.; Wuthrich, K. *J. Mol. Graphics* **1996**, *14*, 51.
(81) Kraulis, P. J. *J Appl. Crystallogr*. **1991**, *24*, 946.

CR940325W